frontiers | Frontiers in Energy Research

TYPE Mini Review
PUBLISHED 03 October 2022
DOI 10.3389/fenrg.2022.982269

OPEN ACCESS

EDITED BY
M.A. Mujtaba,
University of Engineering and Technology, Pakistan

REVIEWED BY
Fahad Noor,
University of Engineering and Technology, Pakistan
Manzoore Elahi Soudagar,
Chandigarh University, India
Muhammad Amjad,
University of Engineering and Technology, Pakistan

*CORRESPONDENCE
Fares Almomani,
falmomani@qu.edu.qa

SPECIALTY SECTION
This article was submitted to Bioenergy and Biofuels, a section of the journal Frontiers in Energy Research

RECEIVED 30 June 2022
ACCEPTED 06 September 2022
PUBLISHED 03 October 2022

CITATION
Rony ZI, Mofijur M, Ahmed SF, Kabir Z, Chowdhury AA and Almomani F (2022), Recent advances in the solar thermochemical splitting of carbon dioxide into synthetic fuels. *Front. Energy Res.* 10:982269. doi: 10.3389/fenrg.2022.982269

Recent advances in the solar thermochemical splitting of carbon dioxide into synthetic fuels

Zahidul Islam Rony[1], M. Mofijur[2,3], Shams Forruque Ahmed[4], Zobaidul Kabir[5], Ashfaque Ahmed Chowdhury[1] and Fares Almomani[6*]

[1]School of Engineering and Technology, Central Queensland University, Rockhampton, QLD, Australia, [2]Centre for Technology in Water and Wastewater, School of Civil and Environmental Engineering, University of Technology Sydney, Ultimo, NSW, Australia, [3]Mechanical Engineering Department, Prince Mohammad Bin Fahd University, Al Khobar, Saudi Arabia, [4]Science and Math Program, Asian University for Women, Chattogram, Bangladesh, [5]School of Environmental and Life Sciences, University of Newcastle, Newcastle Upon Tyne, VA, Australia, [6]Department of Chemical Engineering, Qatar University, Doha, Qatar

Recent years have seen a sharp rise in CO_2 emissions into the atmosphere, which has contributed to the issue of global warming. In response to this several technologies have been developed to convert CO_2 into fuel. It is discovered that the employment of a solar-driven thermochemical process (S-DTCP) that transforms CO_2 into fuels can increase the efficiency of the production of sustainable fuels. The process involves the reduction of metal oxide (MO) and oxidizing it with CO_2 in a two-step process using concentrated solar power (CSP) at higher and lower temperatures, respectively. This study summarizes current advancements in CO_2 conversion methods based on MO thermochemical cycles (ThCy), including their operating parameters, types of cycles, and working principles. It was revealed that the efficiency of the solar conversion of CO_2 to fuel is not only influenced by the composition of the MO, but also by its morphology as well as the available surface area for solid/gas reactions and the diffusion length. The conversion mechanism is governed by surface reaction, which is influenced by these two parameters (diffusion length and specific surface area). Solar energy contributes to the reduction and oxidation steps by promoting reaction kinetics and heat and mass transport in the material. The information on recent advances in metal oxide-based carbon dioxide conversion into fuels will be beneficial to both the industrial and academic sectors of the economy.

KEYWORDS

thermochemical splitting, ceria, perovskites, carbon dioxide emission, climate change

Abbreviations: CO_2, Carbon Dioxide; CO, Carbon monoxide; H^2, Hydrogen; ZnO, Zinc oxide; CeO2, Ceria Oxide; TPO, Temperature-Programmed Oxidation; MS, MassSpectroscopy; SCS, Solution Combustion Synthesis; TR, Thermal Reduction.

1 Introduction

Fossil fuels provide a significant amount of energy (Mofijur et al., 2013a), but their ongoing usage for industrial purposes is threatening the atmosphere because of the high amounts of greenhouse gas emissions i.e. CO_2 (Mofijur et al., 2013b). The impacts of greenhouse gases are widely acknowledged to be one of the fundamental causes of climate change (Langford, 2005). In order to mitigate climate change, it is necessary to minimize the emission of CO_2 (Jacobson et al., 2019). Carbon dioxide is a colorless, naturally occurring gas that is made up of molecules that each have one carbon atom covalently double bonded to two oxygen. Carbon dioxide, in addition to other greenhouse gases, is a significant contributor to the ability of the earth to sustain a temperature that is suitable for human habitation (Garba et al., 2021). Carbon dioxide at low concentrations has less toxicological effect. It causes the development of hypercapnia and respiratory acidosis when more than 5% are present in the atmosphere (Kettner et al., 2013). As a result of the increased effects of parasympathetic nerve activity, which is thought to be caused by interfering with the breakdown of acetylcholine by acetylcholinesterase, severe acidosis can result in a decrease in the rate of respiration (Permentier et al., 2017).

More than 10% of carbon dioxide concentrations have been shown to produce convulsions, coma, and even death (Żaba et al., 2011). Increased CO_2 levels of more than 30% act quickly and can cause loss of consciousness in a matter of seconds. This might explain why sufferers of unintentional intoxication frequently do not act to fix the problem. Capturing carbon dioxide emissions at the site of emission is an appealing concept that has gained popularity in recent years and converting it into useful products such as synthetic fuels (Helal et al., 2020), with the entire cycle being powered by renewable resources such as solar irradiation (Glenk and Reichelstein, 2019). Figure 1 presents the different S-DTCPs used to produce industrial items and fuels. In general, these processes can be divided into two categories: the creation of industrial items and the generation of fuels (Mustafa et al., 2020). Solar fuels are a particularly tempting alternative to non-renewable fossil fuels because of the availability of solar energy and the fact that the production cycle produces almost no emissions (Shahabuddin et al., 2021). The method of manufacturing solar fuels generally comprises (i) thermochemical reduction-oxidation (redox) splitting of plentiful CO_2/H_2O into a CO/H_2 known as syngas; and (ii) hydrocarbon fuel synthesis by some well-established gas to liquid

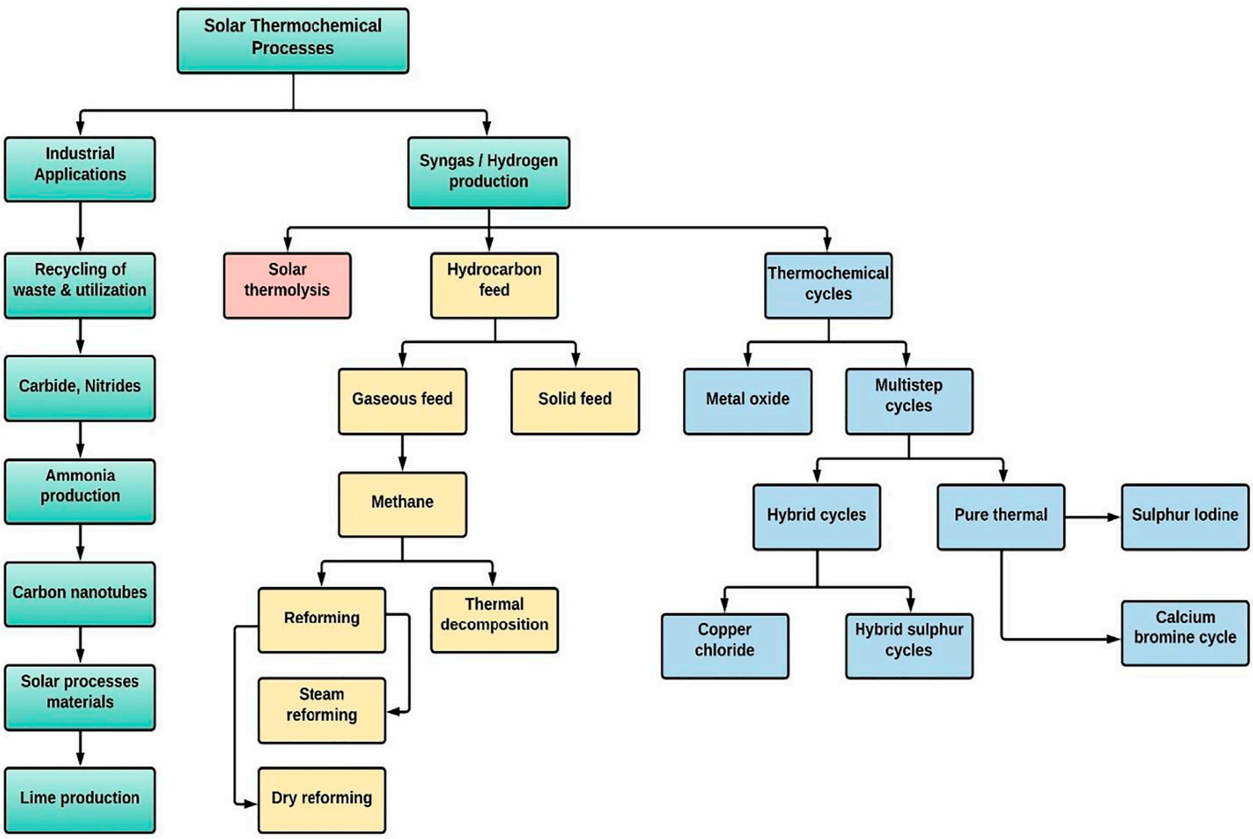

FIGURE 1
List of thermochemical processes that use solar energy to produce industry items and fuels (Mustafa et al., 2020).

processes (e.g. Fischer–Tropsch). In contrast, the commercialisation of solar-powered syngas has not yet been realised, mostly as a result of the process's low solar-to-fuel efficiency (Boretti, 2021).

The development of redox materials has received increased attention in recent years, intending to increase the efficiency of the technology while also making it more financially viable (Scheffe and Steinfeld, 2014). The ability of a redox material to exchange oxygen (release/absorption of O_2) has a direct and proportional impact on the amount per mass of material. The use of redox materials in solar fuel production processes has proven successful in the past. Oxide minerals such as ferrites (Kodama et al., 2005; Scheffe et al., 2013a) and hercynite (Arifin et al., 2012; Muhich et al., 2013), and more recently ceria (Chueh et al., 2010; Furler et al., 2012a) and perovskites (Cooper et al., 2015; Dey et al., 2015a; Ezbiri et al., 2017a; Takacs et al., 2016), have been used successfully as redox materials (Boretti et al., 2021). It is evidenced that many pieces of researches are published on thermochemical splitting of CO_2 but few researchers reviewed and analysed them.

Based on the aforementioned literature review, this min review aimed at summarizing the most recent works that are focused on MO-based solar thermochemical CO_2 splitting to fuel. This condensed review will provide researchers updated news about the research directions in this topic and discuss it's the technology readiness level as well as provide recent updates about scientific and industrial aspect of this technology.

2 Solar thermochemical splitting of carbon dioxide via MO-based reaction

It is possible to operate at moderate temperatures and avoid separation difficulties by dissociating CO_2 in many steps, each of which makes use of metal oxides during the redox processes (Snoeckx and Bogaerts, 2017). The first phase is endothermic, and it involves the reduction of oxidized MO (MO_{ox}) to metal (M) or reduced MO (MO_{red}) using solar thermal energy. In the second phase, the MO_{red} is oxidised with CO_2, resulting in the generation of CO. The MO_{ox} can be used again for the first step (Mustafa et al., 2020). Multiple redox cycles are known to exist that can be followed in order to separate H_2O from CO_2. Theoretically, these redox cycles have an efficiency of greater than 40%, according to the researchers. It is generally accepted that two-cycle classes of metal oxides, both volatile and non-volatile, should be considered (Scheffe and Steinfeld, 2014). Doping techniques are used in both types of cycles to improve the thermodynamic, kinetic, and physical properties.

The basic equations for this cycle are:

$$MO_{ox} \rightarrow MO_{red} + O_2 \tag{1}$$

$$MO_{red} + CO_2 \rightarrow MO_{ox} + CO \tag{2}$$

Deepak and Banerjee presented literature that analysis the thermal efficiency of the ThCy on iron and Ceria under different conditions. It was concluded that the thermal efficiency $\left(\frac{\Delta H_{water}}{Q_{total}+P_{H2_{compression}}}\right)$ in the temperature range 600–2300 ranged from 35 to 70% without any heat recovery. The global sun-to H_2 efficiencies for iron and zinc oxide are estimated to be within the ranges at 43–65.2% and 31.6–61.8%, respectively. The variations in the thermal efficiencies were related to the considerations of the optical efficiency of the heliostat field and the thermal efficiency of the reactor. For ceria-based solar ThCy was determined to be in the range of 20.2%–29.5% without heat recovery and increase to 50% with heat recovery A second law analysis was used to examine the exergy efficiency of the ceria-based ThCy as 23% and 26% for reactors operating temperature of 2300 K and 2600 K, respectively

2.1 Solar thermochemical splitting of carbon dioxide via ceria-based redox reactions

Ceria (CeO_2)-based ThCy may be able to store intermittent and diluted solar energy by generating chemical fuels. Many researchers have experimented with and reported the performance of ceria-based ThCy. For example, Hathaway, Bala Chandran, Gladen, Chase, Davidson (Hathaway et al., 2016) et al. studied a 4.4 kW solar receiver/reactor's ability to split CO_2 through the isothermal CeO_2 thermochemical redox cycle in the course of steady-state operation within a high-flux solar simulator. At 1750K, a steady-periodic operation took place where 360 ml min^{-1} of CO generated more than 45 redox cycles in a continuous flow. A 95% of the sensible heat derived from process gases was recovered. Without considering the energy costs of N_2 production, the solar-to-fuel efficiency was 1.64%. N_2 is used as a sweep gas for reduction. Including the solar energy needed for N_2 production through cryogenic separation, the solar-to-fuel efficiency was found to be 0.72%. A conclusion was reached that splitting CO_2 or water, following the isothermal approach, via a thermochemical MO redox cycle does not show prospects for development. There are certain thermodynamic limitations in this cycle and other issues like the inability to increase reactor efficiency beyond 2%.

Lin, Samson, Wismer, Grolimund, Alxneit, Wokaun (Lin et al., 2016) investigated the dual-phase Zn that was modified by ceria synthesized via coprecipitation to be used as a redox material to thermochemically split H_2O and CO_2. In the first few cycles, it was observed that the materials showed a significant increase in the productivity of H_2 and CO. There was a correlation between the increased productivity in the initial cycles and a considerable loss of Zn during the sublimation of ZnO. His observation suggests that the secondary ZnO phase in Zn-modified ceria expressed a negative effect on its thermochemical activity.

Nair, Abanades (Nair and Abanades, 2016a) studied the combination of methane being partially oxidized with the splitting of H_2O and CO_2 set in solar thermal conditions. CO_2 and H_2O were split by CeO_2 by utilizing concentrated solar energy. The reaction temperatures were varying from 900 to 1100 °C. This experiment took place inside a solar-powered thermogravimetric system and results showed close reaction orders of both CO_2-induced oxidation of $CeO_2^{-\delta}$ and CH_4-induced reduction with corresponding activation energies, 36 and 109 kJ mol^{-1}. A comparison of the outcomes was noted down with the ones acquired from surfactant-induced self-assembly and hydrothermal templating. The material synthesis that occurred via hydrothermal and self-assembly methods had high reaction rates and stability on cycling. MgO promoted CeO_2 resulted in a higher rate of reduction and highest nonstoichiometric (δ = 0.431) when reduction occurred at a temperature of 1000°C. Results about the amount of evolved CO implied that reoxidation is almost complete as it came out to be the highest (δ = 0.402). For thermal reduction of ceria, the obtained nonstoichiometric and consequent fuel effectivity were 10 times more than the values that were reported. Some studies were performed in solar reactor prototypes to enable partial ceria reduction in the presence of methane. Subsequently, oxidation with ceria was promoted by H_2O/CO_2. MgO and Al_2O_3 took place and were experimented with under packed bed conditions. This was put into comparison with commercial ceria based on the production of syngas. MgO promoted CeO_2 showed remarkable augmentation in the system efficiency.

Haeussler, Abanades, Julbe, Jouannaux, Cartoixa (Haeussler et al., 2020) designed, constructed and experimented with a new solar reactor that is monolithic and has compatibility with ceria redox reactions when the solar radiation is concentrated. The ceria redox material is built as structures that are porous and reticulated with controlled cell sizes and gradients, 10–60 pores per inch (ppi). These features allow effective volumetric solar radiation absorption and microscale interconnected porosity. This system helps increase efficiency in solid-gas reactions. The effect of functioning conditions like the type of oxidizing gas, pressure and reduction and oxidation temperatures on reactor performance was examined. When the temperature for reduction was increased or the pressure was decreased, the yields of fuel production and ceria reduction extent improved (up to 341 μmol/g). Decreasing CO: CO_2, by raising the total inlet gas flow rate, or increasing inlet CO_2 concentration resulted in an improved rate of oxidation by as far as 9.3 ml/g/min. The observed fuel production rates surpassed the maximum of the previously recorded values 8 times more utilizing the ceria porous foams that were manufactured to be highly reactive that underwent cycling between 900°C and 1400°C. In 100% of CO_2, oxidation took place upon dynamic cooling. A mean H_2/CO production of ~280 Ncm (Langford, 2005)/cycle was attained where 64 cycles were performed, where solar-to-fuel efficiency reached ~7.5% with significant performance stability of the material.

Riaz, Ali, Enge, Tsuzuki, Lowe, Lipiski (Riaz et al., 2020) investigated the effects of the concentrations of two elements, V and Ce, in vanadia–ceria multiphase systems for the generation of synthesis gas through the splitting of CO_2 and H_2O following thermochemical redox cycles of splitting that had methane partial oxidation reactions integrated with it. The concentration range varied from 0 to 100% each. Prepared oxygen carriers' oxidation is executed by separate and sequential splitting reactions of CO_2 and H_2O. Pure CeO_2 showed the lowest oxygen exchange capacities while pure V_2O_5 showed the highest. Pure CeO_2 also exhibited the lowest performance of syngas production whereas pure V_2O_5 showed the highest. The systems involving mixed-oxide showed a balanced neutral performance where the oxygen exchange capacity was recorded to be 5 times higher than what pure CeO_2 shows when the length of methane cracking was decreased. Having 25% V added to CeO_2 resulted in a $CeVO_4$ and CeO_2 optimum mixture for the improved splitting of CO_2 and H_2O. When the concentration of V is high, the formation of cyclic carbide and oxidation are consequent to a syngas yield that is greater than pure CeO_2. The synthesis methods used in preparation of ceria based material is presented in Table 1.

It can be seen that both binary and ternary MOs containing Ce and other metals at different compositions can be utilized in ThCy. Table 2 illustrates the O_2 and H_2/CO productivities of binary and ternary ceria-based composites in multiple solar ThCys. It was discovered that adding some dopants increased the ceria-based material's reactivity and thermal stability through a number of ThCyas.

2.2 Solar thermochemical splitting of carbon dioxide via perovskite-based redox reactions

Perovskites have the capability of providing high production of O_2 at temperatures that are comparatively high (Demont et al., 2014). Additionally, they can integrate reduction oxidation that demands energy (Sastre et al., 2017a). The cation found in the M site determines the redox properties of perovskites. It is denoted by $ABO_3^{-\delta}$ and falls in the category of nonstoichiometric oxides (Mustafa et al., 2020). There has not been much investigation into these oxides to reduce metals in thermochemical cycles (Arshad et al., 2021). The cation sites, A and B, are where the replacement of dopants can take place. This makes material configurations notably larger inside perovskites relative to ceria. Research related to thermodynamics that involved oxygen non-stoichiometry data evaluation and extracting entropies and enthalpies have proven lanthanum strontium manganite perovskites' (indicated by La1-xSrxMn$O_3^{-\delta}$) capability in augmenting oxygen exchange capacity relative to pure ceria

TABLE 1 Experimental findings reported in case of CeO2 based solar thermochemical H2O/CO2 splitting cycles. Reprinted with permission.

Synthesis approach	Cycles	Reduction temperature (°C)	Average O_2 released (μmol/g)	Re-oxidation temperature (°C)	Average H_2 produced (μmol/g)	Average CO produced (μmol/g)	Reference
Commercial	1	2000	–	550	3254	–	Abanades and Flamant, (2006)
Combustion	12	1500	49.55	1000	33.9	–	Kaneko et al. (2008)
Commercial	1	1600	263.4	800	526	–	Abanades et al. (2010)
	500	1500	133.9	800	267	–	
Commercial	4	1581-1624	96.4	900	–	175	Chueh et al. (2010)
	4	1622-1640	118.3	900	188.9	–	
Co-precipitation	3	1400	50	1000-1200	–	100	Meng et al. (2011)
	3	1400	70	1000-1200	–	–	
Polymerized complex	4	1500	27	500	–	–	Le Gal et al. (2011)
Polymerized complex	9	1500	79.1	500	142.4	–	Petkovich et al. (2011)
Commercial	10	1494-1582	67.9	927	98.66	41	Lapp et al. (2012)
Commercial	1	1597	100.8	–	–	203	Bader et al. (2013)
Auto- combustion	22	1500	55.8	1500	87.5	–	Call et al. (2013)
Commercial	2	1400	80	1050	120	–	Hao et al. (2013)
Hydrothermal	1	1500	254.5	800	–	348	Kang et al. (2014)
Electrospinning	10	1200	–	800	–	18	Scheffe et al. (2013c)
50 vol% pore-forming agent	20	1500	–	1000	–	199.6	Furler et al. (2014)
30 vol% pore-forming agent	1	1574	112.5	–	–	224	Furler et al. (2014)
Complex polymerization	9	1500	69.2	500	–	–	Cho et al. (2015)
Commercial Replication	1	1547	97.3	–	–	196.9	Marxer et al. (2015)
Commercial	2	1500	130	1000	–	240	Zhao et al. (2016)
Commercial	3	1400	30	1000	–	60	Zhao et al. (2016)
Co-precipitation	4	1290	–	1000	50	–	Gao et al. (2016)
	4	1400	–	1000	–	90	

(Scheffe et al., 2013b). It has been experimentally confirmed that even though the extent of reduction is notably higher, oxidation is thermodynamically less viable and this causes oxidation to be incomplete. Nevertheless, total CO generation from the decomposition of CO_2 continues to be significantly higher in contrast to ceria.

Perovskites are considered to be potential redox materials for fuel synthesis via thermo-electrochemical means Ezbiri, Takacs, Stolz, Lungthok, Steinfeld, Michalsky (Ezbiri et al., 2017b). For designing perovskites that constitute balanced redox energetics for the thermochemical splitting of CO_2, electronic structure computations predict lattice oxygen vacancy activities as well as the stability of a representative range of perovskites against phase changes of crystals and deleterious carbonate formation (Rafique et al., 2022). The range of free energy calculated for isothermal and temperature-swing redox cycles is used for illustrating systematic changes in the characteristics of these materials when they have specific metal cations doped with them.

Mulmi, Chen, Hassan, Marco, Berry, Sharif, Slater, Roberts, Adams, Thangadurai (Mulmi et al., 2017) examined the usage of perovskite oxides that are nonstoichiometric, ($Ba_2Ca0.66Nb1.34{-}xFexO_6^{-\delta}$ (BCNF) ($0 \leq x \leq 1$)), for the purpose of splitting CO_2 into C, CO, and O_2 at increased temperatures. Double perovskite-type BCNF's chemical stability is exhibited by powder X-ray diffraction after exposure to CO_2 of 2000 ppm in Ar at a

TABLE 2 Experimental findings reported in case of doped ceria based solar thermochemical H2O/CO2 splitting cycles. Reprinted with permission from Bhosale et al. (2019)

Dopant concentration	Synthesis approach	Cycles	Reduction temperature (°C)	Average O_2 released (μmol/g)	Re-oxidation temperature (°C)	Average H_2 produced (μmol/g)	Average CO produced (μmol/g)	Reference
10% Mn	Combustion	1	1500	80	1000	168.3	–	Roeb et al. (2012)
10% Ni	Combustion	1	1500	115.2	1000	121.8	-	
10% Cu	Combustion	1	1500	69.6	1000	43.8	-	
10% Fe	Combustion	4	1400	59.4	1000	100.9	-	
11% Fe	Combustion	11	1400	58.03	1000	89	-	Charvin et al. (2009)
75% Zr	Co-precipitation	4	1400	–	1100	26	-	Kaneko and Tamaura, (2009)
		1	1400	–	1100	–	158.5	
50% Si	Co-melting	1	1500	1110	530	1500-1940	–	Miller et al. (2008)
50% Ti	Co-melting	1	1400	1000	630	1560-1740	–	
50% Fe	Co-melting	1	1400-1500	1000	500	600	–	
50% Nb	Co-melting	1	700	840	500	820	–	
5% Ni	Combustion	8	1400	62.5	1000	89	–	Chueh and Haile, (2010)
15% Sm	Commercial	53	–	–	700	343.8	–	Chueh and Haile, (2009)
10% Ni 15% Sm	Wetness impregnation	11	–	–	500	151.8	10.3	
25% Zr	Pechini	2	1450	110	950	130	–	Le Gal and Abanades, (2011)
25% Zr	Co-precipitation	2	1400	180	1050	320	–	Kaneko et al. (2011)
25% Zr	Pechini	3	1400	140	1000-1200	–	200	Meng et al. (2011)
		3	1400	220	1000-1200	380	–	
20% Zr	Polymerized complex	4	1500	129.5	500	–	–	Le Gal et al. (2011)
10% Mg	Polymerized complex	9	1500	88.4	500	173.9	–	Petkovich et al. (2011)
10% Sc	Polymerized complex	9	1500	98.7	500	181	–	
10% Hf	Polymerized complex	9	1500	132	500	200.9	–	
10% Pr	Combustion	1	1500	104	750	177	–	Furler et al. (2012b)
2.5% Li	Polymerized complex	9	1500	1300	500	2400	–	Le Gal and Abanades, (2012)
10% Ta	Co-precipitation	1	1450	–	1040	140	–	
25% Ta	Co-precipitation	2	1400	–	1050	70	–	
10% La	Co-precipitation	3	1400	60-100	1000-1200	120-140	–	
10% Sm	Co-precipitation	2	1400	60	1050	110	–	
10% Gd	Co-precipitation	2	1400	60	1050	100	–	
25% Zr	Co-precipitation	2	1400	170	1050	270	–	
23% Zr 2% La	Co-precipitation	2	1400	140	1050	260	–	
23% Zr 2% Y	Co-precipitation	2	1400	150	1050	240	–	
25% Zr 1% Gd	Co-precipitation	2	1400	190	1050	280	–	
25% Zr	Co-precipitation	2	1450	140	950	–	120	Furler et al. (2012a)
10% Zr	Co-precipitation	2	1400	90	1050	–	120	
25% Zr	Pechini	3	1400	120-180	1000-1200	–	140-240	

(Continued on following page)

TABLE 2 (*Continued*) Experimental findings reported in case of doped ceria based solar thermochemical H2O/CO2 splitting cycles. Reprinted with permission from Bhosale et al. (2019)

Dopant concentration	Synthesis approach	Cycles	Reduction temperature (°C)	Average O_2 released (μmol/g)	Re-oxidation temperature (°C)	Average H_2 produced (μmol/g)	Average CO produced (μmol/g)	Reference
54% Zr	Commercial	2	1400	230	1050	390	–	Hao et al. (2013)
50% Zr	Co-precipitation	2	1400	230	1050	370	–	
37% Zr	Pechini	2	1400	210	1050	370	–	
24% Zr	Pechini	2	1400	190	1050	340	–	
1% Gd 40% Zr	Commercial	2	1300	150	1050	290	–	
15% Zr	Auto-combustion	4	1400	160	900	–	310	Scheffe et al. (2013d)
15% Zr	Auto-combustion	100	1400	100-150	900	–	200-280	
20% Zr	Co-precipitation	2	1400	116	1100	–	192.42	Meng and Tamaura, (2014)
10% Ni 20% Zr	Co-precipitation	2	1400	158.5	1100	–	135.7	
10% Fe 20% Zr	Co-precipitation	2	1400	184.4	1100	–	165.2	
10% Mg 20% Zr	Co-precipitation	2	1400	140	1100	–	241.5	
10% Mn 20% Zr	Co-precipitation	2	1400	249	1100	–	102.2	
2% Mg 20% Zr	Co-precipitation	2	1400	296.9	1100	–	282.1	
10% Hf 10% Pr	Polymerized complex	5	1500	137.9	500	255.3	–	Jiang et al. (2014)
20% Ti	Co-precipitation	1	1400	589	900	–	53.6	Kang et al. (2014)
25% Hf	Hydrothermal	1	1400	321.4	1000	–	111.6	
15% La	Hydrothermal	1	1500	321.4	800	–	272	
25% Zr	Combustion	1	1400	290.2	900	–	473.2	
20% Sn	Combustion	1	1400	500	–	–	–	
15% Sm	Hydrothermal	1	1500	169.4	–	–	–	
15% Y	Hydrothermal	1	1500	174	–	–	–	
10% Mg 20% Zr	Hydrothermal	3	1400	135.7	1100	–	232.6	Jiang et al. (2014)
5% Ca 20% Zr	Hydrothermal	3	1400	160	1100	–	282.5	
5% Mg 20% Zr	Hydrothermal	2	1200	60.7	1000	–	107	
5% Ca 20% Zr	Hydrothermal	2	1200	70.1	1000	–	137.0	
10% Zr	Electrospinning	10	1140	–	740	–	71.4	Scheffe et al. (2013c)
2.5% Zr	Electrospinning	108	1400	–	800	–	178	
10% Dy	Complex polymerization	9	1500	48.2	500	–	–	
10% Y	Complex polymerization	9	1500	51.3	500	–	–	
10% Sc	Complex polymerization	9	1500	83	500	–	–	
10% Zr	Complex polymerization	9	1500	108.9	500	–	–	

(Continued on following page)

TABLE 2 (*Continued*) Experimental findings reported in case of doped ceria based solar thermochemical H2O/CO2 splitting cycles. Reprinted with permission from Bhosale et al. (2019)

Dopant concentration	Synthesis approach	Cycles	Reduction temperature (°C)	Average O_2 released (μmol/g)	Re-oxidation temperature (°C)	Average H_2 produced (μmol/g)	Average CO produced (μmol/g)	Reference
10% Hf	Complex polymerization	9	1500	137	500	–	–	
15% Zr	Auto-combustion	4	1400	160	900	–	310	
2.5% Sm	Auto-combustion	4	1400	150	900	–	300	
15% Zr								
2.5% Y	Auto-combustion	4	1400	140	900	–	260	
15% Zr								
2.5% La	Auto-combustion	4	1400	140	900	–	270	
15% Zr								
2.5% Gd	Auto-combustion	4	1400	140	900	–	270	
15% Zr								
10% Zr	Solid state reaction	2	1500	160	1000	–	330	Zhao et al. (2016)
20% Hf	Solid state reaction	2	1500	230	1000	–	390	
2% Li	Solid state reaction	2	1500	170	1000	–	340	
9.8% Hf								
50% Zr	Co-precipitation	3	1400	140	1000	–	270	Zhao et al. (2016)
2% Pr	Co-precipitation	3	1400	140	1000	–	290	
8% La								
50% Zr								
50% Fe	Sol-gel	8	1400	70	1000	–	120	Bhosale et al. (2016)
5% Zr	Co-precipitation	4	1400	120	1000	–	170	
5% Hf								
5% Zr	Co-precipitation	20	1400	110	1000	–	160-	
5% Hf								
20% Zn	Co-precipitation	4	1290	–	1000	20–60		
		4	1400	–	1000	–	60-110	
1% Rh	Co-precipitation	6	1400	74	500	130	–	
		59	1400	80	500	150	–	
		11	1500	120	500	200	–	
50% Mg	Solid solution	3	1000	1850	1000	–	1720	
50% Al	Solid solution	3	1000	1130	1000	–	1100	

temperature of 700°C. All members of $x \leq 0.66$ BCNF express great chemical stability despite being in conditions at 700 °C temperature and pure CO_2. The creation of solid carbon upon being exposed to CO_2 was confirmed through scanning electron microscopy along with Raman spectroscopy, DFT analyses, temperature-programmed oxidation (TPO) and mass spectroscopy (MS), and energy-dispersive X-ray. As Fe increases, more solid carbon is produced in BCNF. In the Mössbauer spectroscopy of the as-prepared BCNF, Fe^{3+}, Fe^{4+} and Fe^{5+} were found. When exposed to Ar, a constituent Fe that has higher valence undergoes reduction to Fe^{3+} followed by Fe^{3+} enhanced CO_2 reduction being oxidized. The overall outcomes of BCNFs displayed redox activity at much lesser temperatures if put into comparison with state-of-the-art ceria for reducing CO_2. Thus, it can be seen that there is a possibility of putting them into use in fuel technologies that are powered by renewable sources.

Sastre, Carrillo, Serrano, Pizarro, Coronado (Sastre et al., 2017b) proposed mixed oxides with perovskite structure as an alternate material for solar fuel generation through thermochemical redox cycles. The system La0.6Sr0.4Mn1−xAlxO_3 (x = 0–0.8) was chosen for this study as it has the required features: thermal stability that is high and rapid oxidation kinetics. The ratio of Al/Mn and its impact on the redox properties were also looked into. After characterization through thermogravimetric analysis, the five oxides samples having varying Al amounts verified the high redox capacity. They also verified the favourable behaviour of these materials in consecutive cycles. According to the results, consequent of reduction at temperature 1300 °C in the inert atmosphere, there is a release of up to 0.32 mmol g^{-1} of O_2. A reaction test of 10 cycles confirmed that for long-term operations, perovskites are viable. Based on observations, when the content of Al was increased, the reduction extent became enhanced. However, the oxidation degree is maximal for constitutions that are close to x = 0.5 and showed 0.318 mmol g^{-1} O_2 delivery ($\delta = 0.132$). After the selection of the constitutions having potentially better redox properties, further reactions were operated in a fixed bed reactor that is of lab scale. For CO formation, CO_2 was injected in the oxidation step at 900°C. Perovskite La0.6Sr0.4Mn0.6Al0.4O_3 showed interesting results where the reduction extent was 0.266 mmol g^{-1}. However, CO generation is comparatively notably lower with the value being 0.114 mmol g^{-1}.

Ramos, Maiti, Daza, Kuhn, Bhethanabotla (Ramos et al., 2019) assert that perovskite oxides in the category of type ABO_3 have proven significant potential for thermochemical CO_2 conversion at low temperature using the reverse water gas shift chemical looping (RWGS-CL) process. Transition metals on the 'B' site of these perovskite oxides are responsible for adjusting the material properties necessary for the effective conversion of CO_2. The functions of Fe, Mn and Co in $LaBO_3$ were explored using an integrated approach of both theory and experiment. Ab-initio density functional theory (DFT) simulations were used for investigating the intrinsic oxygen vacancy generation features and electronic charge distribution of these materials. Properties that are microscale including conversion yield of CO_2 and crystallite size were explored by experiments. A comparative analysis is performed to differentiate the material properties influencing the stability and improved CO_2 conversion process using perovskites that are plentiful in Fe, in contrast to Mn and Co-rich phases.

Parvanian, Salimijazi, Shabaninejad, Troitzsch, Kreider, Lipiński, Saadatfar (Parvanian et al., 2020) explored the redox functioning ability of porous ceramics having a coating of perovskite designing different forms of architecture. Fabrication of reticulated porous ceramics (RPCs) in three varying pore sizes was done for representing structures and pore sizes of a wide range. The pore sizes were 5, 12, and 75 ppi. The perovskite matter is composed of lanthanum manganite. After its synthesis, the perovskite material underwent Ca and Al doping via Pechini method. Implementing a method involving deep coating, the surface of RPC substrates underwent modifications and got a thin-film coating with ~15 μm thickness. The CO_2 conversion performance of the materials that were formed was evaluated in a gold-image IR furnace. For an in-depth investigation of features pertaining to bulk and surface, an X-ray micro-computed tomography along with SEM/EDX was employed during the investigation. According to findings, 12 ppi, which is the intermediate pore size, reaches the highest perovskite loading and shows a high level of coating uniformity and connectivity. The highest CO generation for 75 ppi was observed after CO_2 conversion tests. Inside the furnace, the severe conditions, along with the flow of gaseous phases make the RPCs shrink to 23% of their original length. This alters the pore phase and eliminates minute pores thus decreasing the overall specific surface area. The findings also revealed a major mechanism that causes the CO_2 conversion to stop where the coating layer of perovskite shifts its position into the matrix of the RPC frame.

Takalkar, Bhosale, AlMomani, Rashid, Qiblawey, Saleh Saad, Khraisheh, Kumar, Gupta, Shende (Takalkar et al., 2021) investigated La (1-x) SrxMnO_3 (LSM) perovskites and their redox reactivity in the context of splitting CO_2. Synthesis of LSM perovskites took place following the solution combustion synthesis (SCS) technique. This technique used glycine as a reducing agent. Many types of analytical approaches are used to characterize the structural properties of LSM perovskites. In three sets, thermogravimetric thermal reduction (TR) and CS cycles are conducted to acquire an estimation of the amount of O_2 released (nO_2) and CO yielded (nCO) by an individual lanthanum strontium manganite perovskite. The sets are in one, three and ten cycles. Higher nO_2 by each LSM perovskite is released than the nCO that releases nO_2 during the first cycle. The nO_2 is lessened, and each LSM perovskite's re-oxidation capacity is enhanced from cycle one to cycle three. Considering the average n_{O2} and $n_{CO}$from cycle 2-cycle 10, the perovskites La0.30Sr0.70Mn0.99O_2.982 (342.1 μmol of CO/g. cycle) and La0.60Sr0.41Mn0.99O2.993 (214.8 μmol of O_2/g·cycle) have been found to reach the top highest redox reactivity. LSM perovskites, excluding La0.88Sr0.11Mn1.00O_2.980, have a record of having a very high redox activity than the CeO_2 material.

There are a large number of studies that are based on perovskite-based redox reactions as presented in Table 3 in the supplementary documents. It was concluded that although perovskite-based redox reactions can accommodate a wide range of oxygen, the high vacancy formation associated with re-oxidation stem imped the reaction and generated low ratio of CO/H_2. There for a compromises between maximal achievable oxygen and fuel generation yield should be optimized, which can be controlled by perovskite formulation.

Challenges for solar thermochemical processes

The challenges connected to various solar thermochemical processes can be summarized as follow:

1 The primary disadvantage of using perovskites is typically the insufficient re-oxidation yield brought on by low kinetics

TABLE 3 Summary of the thermochemical cycles based on perovskites studies. Reprinted with permission from Bhosale et al. (2019)

Material	Synthesis method	Experimental conditions	O_2Production	H_2/CO	Reference
La0.7Sr0.3Mn0.7Cr0.3O3	Modified Pechini	Reduction: 1350°C under N2 Oxidation: H2O between 50 and 84%; 1000°C during 60 min	~98	~107	Gokon et al. (2019)
LaFe0.75Co0.25O3	Solid-state	Reduction: 1300°C under Ar Oxidation: 50% CO2 in Ar at 1000°C	59	117	Nair Mahesh and Abanades, (2018)
LaCoO3	Solid-state	Reduction: 1300°C under Ar Oxidation: 50% CO2 in Ar at 1000°C	369	123	
Ba0.5Sr0.5FeO3	Solid-state	Reduction: 1000°C under Ar Oxidation: 50% CO2 in Ar at 1000°C	582	136	
La0.6Sr0.4Co0.2Cr0.8O3	Pechini	Reduction: 1200°C under Ar Oxidation: 50% CO2 in Ar at 800°C	–	157	Bork et al. (2015)
La0.4Ca0.6Mn0.6Al0.4O3	Modified Pechini	Reduction: 1400°C under Ar Oxidation: 40% H2O in Ar at 1000°C	231	429	Wang et al. (2017a)
BaCe0.25Mn0.75O3	Modified Pechini	Reduction: 1350°C under Ar Oxidation: 40% H2O in Ar at 1000°C	–	135	Barcellos D et al. (2018)
La0.5Sr0.5MnO3	Solid-state	Reduction: 1400°C under Ar Oxidation: H2O at 1000°C	298	195	Demont et al. (2014)
La0.35Sr0.75MnO3	Commercial powder	Reduction: 1400°C under Ar Oxidation: H2O at 1050°C	166	124	
La0.5Ca0.5MnO3	Solid-state	Reduction: 1400°C under Ar Oxidation: 50% CO2 at 1050°C	311	210	Demont and Abanades, (2015)
La0.5Ba0.5MnO3	Solid-state	Reduction: 1400°C under Ar Oxidation: 50% CO2 at 1050°C	203	185	
La0.5Sr0.5Mn0.4Al0.6O3	Pechini	Reduction: 1400°C under Ar Oxidation: 50% CO2 at 1050°C	246	279	
La0.5Sr0.5Mn0.83Mg0.17O3	Solid-state	Reduction: 1400°C under Ar Oxidation: 50% CO2 at 1050°C	214	209	
La0.5Sr0.5MnO3	Pechini	Reduction: 1400°C under Ar Oxidation: 50% CO2 at 1050°C	256	256	Nair and Abanades, (2016b)
Y0.5Sr0.5MnO3	Pechini	Reduction: 1400°C under Ar Oxidation: 50% CO2 at 1050°C	539	101	
La0.6Sr0.4Mn0.6Al0.4O3	Modified Pechini	Reduction: 1400°C under Ar Oxidation: 40% CO2 at 1000°C	–	307	McDaniel et al. (2013)
La0.6Ca0.4Mn0.6Al0.4O3	Modified Pechini	Reduction: 1240°C under Ar Oxidation: 50% CO2 at 850°C	165	230	Cooper et al. (2015)
La0.6Sr0.4Mn0.6Al0.4O3	Modified Pechini	Reduction: 1240°C under Ar Oxidation: 50% CO2 at 850°C	190	245	
La0.6Ca0.4Mn0.8Ga0.2O3	Modified Pechini	Reduction: 1300°C Oxidation: H2O at 900°C	212	401	Wang et al. (2017b)
La0.5Sr0.5Mn0.95Sc0.05O3	–	Reduction: 1400°C under Ar Oxidation: 40% CO2 at 1100°C	417	545	Dey et al. (2016)
La0.6Sr0.4Mn0.8Fe0.2O3	Modified Pechini	Reduction: 1350°C under N2 Oxidation: CO2 at 1000°C	286	329	Luciani et al. (2018)
La0.6Sr0.4CoO3	Modified Pechini	Reduction: 1300°C Oxidation: 40% H2O at 900°C	718	514	Wang et al. (2018a)
La0.6Ca0.4CoO3	Modified Pechini	Reduction: 1300°C Oxidation: 40% H2O at 900°C	715	587	Wang et al. (2018b)
Y0.5Ca0.5MnO3	Solid state	Reduction: 1400°C Oxidation: CO2 at 1100°C	573	671	Dey et al. (2015b)

and low thermodynamic driving forces. Tuning the redox properties to maximize fuel production is possible thanks to the wide range of perovskite formulations that are possible and the discovery of novel materials.

2 It is crucial to continue making progress in the discovery and characterization of new, higher-performing redox materials that also meet the criteria for desirable thermodynamics, quick reaction kinetics, and crystallographic stability under thermochemical cycling.]

3 The cost projections for ThCy vary greatly and future cost projections are very difficult to make because they depend on a lot of arbitrary and incorrect assumptions. Therefore, well defined cost analysis is required

4 When producing fuel using a flammable redox material like zinc oxide, the dissociation reaction necessitates a very high temperature, which poses problems for the reactor's materials. It has been noted that a sizable amount of zinc recombines with oxygen during the quench process to form zinc oxide, reducing the process' overall effectiveness. To avoid zinc recombination with oxygen, rapid quenching with fine zinc particles is recommended.

5 Recombination is dealt with by non-volatile redox materials like ceria and iron. However, sintering, where the particle size

increases after a few cycles of operation and lowers overall hydrogen yield, is a problem with ferrite-based cycles.

3 Conclusion

The conversion of CO_2 into fuels and chemicals is a potential alternative strategy for addressing both energy and climate change issues simultaneously. There are several technologies available for converting CO_2 into fuel, each of which faces its own set of obstacles when it comes to implementation in the field. A great deal has been accomplished in solar thermochemical technology, and it has emerged as a viable option for harnessing concentrated solar power. Because it makes direct use of solar energy, this technique is both highly beneficial and advantageous when compared to other energy utilisation methods. In industrial applications (i.e. electricity generation), CO_2 and H_2O reduction, concentrated solar energy is increasingly being used. However, even though the thermochemical splitting of CO_2 and H_2O through metal oxides is thermodynamically feasible, further research on achieving higher efficiency is still recommended.

Author contributions

ZR: Writing original draft; MM: Writing original draft; SA: Writing original draft; AC: Review and editing; FA: Review and editing.

Conflict of interest

The authors declare that the research was conducted in the absence of any commercial or financial relationships that could be construed as a potential conflict of interest.

Publisher's note

All claims expressed in this article are solely those of the authors and do not necessarily represent those of their affiliated organizations, or those of the publisher, the editors and the reviewers. Any product that may be evaluated in this article, or claim that may be made by its manufacturer, is not guaranteed or endorsed by the publisher.

References

Abanades, S., and Flamant, G. (2006). Solar hydrogen production from the thermal splitting of methane in a high temperature solar chemical reactor. *Sol. Energy* 80 (10), 1321–1332. doi:10.1016/j.solener.2005.11.004

Abanades, S., Legal, A., Cordier, A., Peraudeau, G., Flamant, G., and Julbe, A. (2010). Investigation of reactive cerium-based oxides for H_2 production by thermochemical two-step water-splitting. *J. Mat. Sci.* 45 (15), 4163–4173. doi:10.1007/s10853-010-4506-4

Arifin, D., Aston, V. J., Liang, X., McDaniel, A. H., and Weimer, A. W. (2012). $CoFe_2O_4$ on a porous Al_2O_3 nanostructure for solar thermochemical CO_2 splitting. *Energy Environ. Sci.* 5, 9438–9443. doi:10.1039/c2ee22090c

Arshad, Z., Khoja, A. H., Shakir, S., Afzal, A., Mujtaba, M. A., Soudagar, M. E. M., et al. (2021). Magnesium doped TiO_2 as an efficient electron transport layer in perovskite solar cells. *Case Stud. Therm. Eng.* 26, 101101. doi:10.1016/j.csite.2021.101101

Bader, R., Venstrom, L. J., Davidson, J. H., and Lipiński, W. (2013). Thermodynamic analysis of isothermal redox cycling of ceria for solar fuel production. *Energy fuels.* 27 (9), 5533–5544. doi:10.1021/ef400132d

Barcellos D, R., Sanders, M. D., Tong, J., McDaniel, A. H., and O'Hayre, R. P. (2018). $BaCe_{0.25}Mn_{0.75}O_{3-\delta}$—A promising perovskite-type oxide for solar thermochemical hydrogen production. *Energy Environ. Sci.* 11 (11), 3256–3265. doi:10.1039/c8ee01989d

Bhosale, R. R., Kumar, A., AlMomani, F., et al. (2016). Assessment of CexZryHfzO2 based oxides as potential solar thermochemical CO2 splitting materials. *Ceram. Int.* 42 (8), 9354. doi:10.1016/j.ceramint.2016.02.100

Bhosale, R. R., Takalkar, G., Sutar, P., Kumar, A., AlMomani, F., and Khraisheh, M. (2019). A decade of ceria based solar thermochemical H2O/CO2 splitting cycle. *Int. J. Hydrog. Energy* 44 (1), 34–60. doi:10.1016/j.ijhydene.2018.04.080

Boretti, A., Castelletto, S., and De Angelis, F. (2021). A solar concentrator/receiver/storage/reactor system for thermochemical splitting cycles based on perovskites. *Int. J. Hydrogen Energy* 47, 4970–4975. doi:10.1016/j.ijhydene.2021.11.094

Boretti, A. (2021). Concentrated solar energy-driven carbon black catalytic thermal decomposition of methane. *Int. J. Energy Res.* 45, 21497–21508. doi:10.1002/er.7142

Bork, A. H., Kubicek, M., Struzik, M., and Rupp, J. L. M. (2015). Perovskite $La_{0.6}Sr_{0.4}Cr_{1-x}Co_xO_{3-\delta}$ solid solutions for solar-thermochemical fuel production: Strategies to lower the operation temperature. *J. Mat. Chem. A Mat.* 3 (30), 15546–15557. doi:10.1039/c5ta02519b

Call, F., Roeb, M., Schmücker, M., Bru, H., Curulla-Ferre, D., Sattler, C., et al. (2013). Thermogravimetric analysis of zirconia-doped ceria for thermochemical production of solar fuel. *Am. J. Anal. Chem.* 2013, 37–45. doi:10.4236/ajac.2013.410a1005

Charvin, P., Abanades, S., Beche, E., Lemont, F., and Flamant, G. (2009). Hydrogen production from mixed cerium oxides via three-step water-splitting cycles. *Solid State Ion.* 14 (180), 1003–1010. doi:10.1016/j.ssi.2009.03.015

Cho, H., Gokon, N., Kodama, T., Kang, Y., and Lee, H. (2015). Improved operation of solar reactor for two-step water-splitting H2 production by ceria-coated ceramic foam device. *Int. J. Hydrogen Energy* 40 (1), 114–124. doi:10.1016/j.ijhydene.2014.10.084

Chueh, W. C., Falter, C., Abbott, M., Scipio, D., Furler, P., Haile, S. M., et al. (2010). High-flux solar-driven thermochemical dissociation of CO_2 and H_2O using nonstoichiometric ceria. *Science* 330, 1797–1801. doi:10.1126/science.1197834

Chueh, W. C., and Haile, S. M. (2010). A thermochemical study of ceria: Exploiting an old material for new modes of energy conversion and CO_2 mitigation. *Phil. Trans. R. Soc. A* 368 (1923), 3269–3294. doi:10.1098/rsta.2010.0114

Chueh, W. C., and Haile, S. M. (2009). Ceria as a thermochemical reaction medium for selectively generating syngas or methane from H_2O and CO_2. *ChemSusChem* 2 (8), 735–739. doi:10.1002/cssc.200900138

Cooper, T., Scheffe, J. R., Galvez, M. E., Jacot, R., Patzke, G., and Steinfeld, A. (2015). Lanthanum manganite perovskites with Ca/Sr A-site and Al B-site doping as effective oxygen exchange materials for solar thermochemical fuel production. *Energy Technol.* 3, 1130–1142. doi:10.1002/ente.201500226

Demont, A., Abanades, S., and Beche, E. (2014). Investigation of perovskite structures as oxygen-exchange redox materials for hydrogen production from thermochemical two-step water-splitting cycles. *J. Phys. Chem. C* 118, 12682–12692. doi:10.1021/jp5034849

Demont, A., and Abanades, S. (2015). Solar thermochemical conversion of CO_2 into fuel via two-step redox cycling of non-stoichiometric Mn-containing perovskite oxides. *J. Mat. Chem. A Mat.* 3 (7), 3536–3546. doi:10.1039/c4ta06655c

Dey, S., Naidu, B. S., Govindaraj, A., and Rao, C. N. R. (2015). Noteworthy performance of $La_{1-x}Ca_xMnO_3$ perovskites in generating H2 and CO by the thermochemical splitting of H_2O and CO_2. *Phys. Chem. Chem. Phys.* 17, 122–125. doi:10.1039/c4cp04578e

Dey, S., Naidu, B. S., and Rao, C. N. R. (2016). Beneficial effects of substituting trivalent ions in the B-site of $La_{0.5}Sr_{0.5}Mn_{1-x}A_xO_3$ (A = Al, Ga, Sc) on the thermochemical generation of CO and H_2 from CO_2 and H_2O. *Dalton Trans.* 45 (6), 2430–2435. doi:10.1039/c5dt04822b

Dey, S., Naidu, B. S., and Rao, C. N. R. (2015). $Ln_{0.5}A_{0.5}MnO_3$ (Ln=Lanthanide, A= Ca, Sr) perovskites exhibiting remarkable performance in the thermochemical generation of CO and H_2 from CO_2 and H_2O. *Chem. Eur. J.* 21 (19), 7077–7081. doi:10.1002/chem.201500442

Ezbiri, M., Takacs, M., Stolz, B., Lungthok, J., Steinfeld, A., and Michalsky, R. (2017). Design principles of perovskites for solar-driven thermochemical splitting of CO_2. *J. Mater. Chem. A* 5, 15105–15115. doi:10.1039/c7ta02081c

Ezbiri, M., Takacs, M., Theiler, D., Michalsky, R., and Steinfeld, A. (2017). Tunable thermodynamic activity of $LaxSr_{1-x}MnyAl_{1-y}O_{3-\delta}$ ($0 \le x \le 1$, $0 \le y \le 1$) perovskites for solar thermochemical fuel synthesis. *J. Mat. Chem. A Mat.* 5, 4172–4182. doi:10.1039/c6ta06644e

Furler, P., Scheffe, J., Gorbar, M., Moes, L., Vogt, U., and Steinfeld, A. (2012). Solar thermochemical CO_2 splitting utilizing a reticulated porous ceria redox system. *Energy fuels.* 26, 7051–7059. doi:10.1021/ef3013757

Furler, P., Scheffe, J., Marxer, D., Michal, G., Bonk, A., Ulrich, V., et al. (2014). Thermochemical CO_2 splitting via redox cycling of ceria reticulated foam structures with dual-scale porosities. *Phys. Chem. Chem. Phys.* 16 (22), 10503–10511. doi:10.1039/C4CP01172D

Furler, P., Scheffe, J. R., and Steinfeld, A. (2012). Syngas production by simultaneous splitting of H_2O and CO_2 via ceria redox reactions in a high-temperature solar reactor. *Energy & Environ. Sci.* 5 (3), 6098–6103. doi:10.1039/C1EE02620H

Gao, X., Vidal, A., Bayon, A., Bader, R., Hinkley, J., Lipinski, W., et al. (2016). Efficient ceria nanostructures for enhanced solar fuel production via high-temperature thermochemical redox cycles. *J. Mat. Chem. A Mat.* 4 (24), 9614–9624. doi:10.1039/c6ta02187e

Garba, M. D., Usman, M., Khan, S., Shehzad, F., Galadima, A., Ehsan, M. F., et al. (2021). CO_2 towards fuels: A review of catalytic conversion of carbon dioxide to hydrocarbons. *J. Environ. Chem. Eng.* 9, 104756. doi:10.1016/j.jece.2020.104756

Glenk, G., and Reichelstein, S. (2019). Economics of converting renewable power to hydrogen. *Nat. Energy* 4, 216–222. doi:10.1038/s41560-019-0326-1

Gokon, N., Hara, K., Sugiyama, Y., Bellan, S., Kodama, T., and Hyun-seok, C. (2019). Thermochemical two-step water splitting cycle using perovskite oxides based on $LaSrMnO_3$ redox system for solar H2 production. *Thermochim. Acta* 680, 178374. doi:10.1016/j.tca.2019.178374

Haeussler, A., Abanades, S., Julbe, A., Jouannaux, J., and Cartoixa, B. (2020). Solar thermochemical fuel production from H_2O and CO_2 splitting via two-step redox cycling of reticulated porous ceria structures integrated in a monolithic cavity-type reactor. *Energy* 201, 117649. doi:10.1016/j.energy.2020.117649

Hao, Y., Yang, C-K., and Haile, S. M. (2013). High-temperature isothermal chemical cycling for solar-driven fuel production. *Phys. Chem. Chem. Phys.* 15 (40), 17084–17092. doi:10.1039/c3cp53270d

Hathaway, B. J., Bala Chandran, R., Gladen, A. C., Chase, T. R., and Davidson, J. H. (2016). Demonstration of a solar reactor for carbon dioxide splitting via the isothermal ceria redox cycle and practical implications. *Energy fuels.* 30, 6654–6661. doi:10.1021/acs.energyfuels.6b01265

Helal, A., Cordova, K. E., Arafat, M. E., Usman, M., and Yamani, Z. H. (2020). Defect-engineering a metal–organic framework for CO_2 fixation in the synthesis of bioactive oxazolidinones. *Inorg. Chem. Front.* 7, 3571–3577. doi:10.1039/d0qi00496k

Jacobson, T. A., Kler, J. S., Hernke, M. T., Braun, R. K., Meyer, K. C., and Funk, W. E. (2019). Direct human health risks of increased atmospheric carbon dioxide. *Nat. Sustain.* 2, 691–701. doi:10.1038/s41893-019-0323-1

Jiang, Q., Zhou, G., Jiang, Z., and Li, C. (2014). Thermochemical CO_2 splitting reaction with CexM1−xO2−δ (M=Ti^{4+}, Sn^{4+}, Hf^{4+}, Zr^{4+}, La^{3+}, Y^{3+} and Sm^{3+}) solid solutions. *Sol. Energy* 99, 55–66. doi:10.1016/j.solener.2013.10.021

Kaneko, H., Ishihara, H., Taku, S., Naganuma, Y., Hasegawa, N., and Tamaura, Y. (2008). Cerium ion redox system in $CeO_{2-x}Fe_2O_3$ solid solution at high temperatures (1, 273–1, 673 K) in the two-step water-splitting reaction for solar H2 generation. *J. Mat. Sci.* 43 (9), 3153–3161. doi:10.1007/s10853-008-2499-z

Kaneko, H., Taku, S., and Tamaura, Y. (2011). Reduction reactivity of CeO_2–ZrO_2 oxide under high O_2 partial pressure in two-step water splitting process. *Sol. Energy* 85 (9), 2321–2330. doi:10.1016/j.solener.2011.06.019

Kaneko, H., and Tamaura, Y. (2009). Reactivity and XAFS study on (1−x) $CeO_{2-x}NiO_{\ (x=\ 0.025-0.3)}$ system in the two-step water-splitting reaction for solar H2 production. *J. Phys. Chem. Solids* 70 (6), 1008–1014. doi:10.1016/j.jpcs.2009.05.015

Kang, M., Wu, X., Zhang, J., Zhao, N., Wei, W., and Sun, Y. (2014). Enhanced thermochemical CO 2 splitting over Mg-and Ca-doped ceria/zirconia solid solutions. *RSC Adv.* 4 (11), 5583–5590. doi:10.1039/c3ra45595e

Kettner, M., Ramsthaler, F., Juhnke, C., Bux, R., and Schmidt, P. (2013). A fatal case of CO(2) intoxication in a fermentation tank. *J. Forensic Sci.* 58, 556–558. doi:10.1111/1556-4029.12058

Kodama, T., Kondoh, Y., Yamamoto, R., Andou, H., and Satou, N. (2005). Thermochemical hydrogen production by a redox system of ZrO_2-supported Co(II)-ferrite. *Sol. Energy* 78, 623–631. doi:10.1016/j.solener.2004.04.008

Langford, N. J. (2005). Carbon dioxide poisoning. *Toxicol. Rev.* 24, 229–235. doi:10.2165/00139709-200524040-00003

Lapp, J., Davidson, J. H., and Lipiński, W. (2012). Efficiency of two-step solar thermochemical non-stoichiometric redox cycles with heat recovery. *Energy* 37 (1), 591–600. doi:10.1016/j.energy.2011.10.045

Le Gal, A., and Abanades, S. (2011). Catalytic investigation of ceria-zirconia solid solutions for solar hydrogen production. *Int. J. Hydrogen Energy* 36 (8), 4739–4748. doi:10.1016/j.ijhydene.2011.01.078

Le Gal, A., and Abanades, S. (2012). Dopant incorporation in ceria for enhanced water-splitting activity during solar thermochemical hydrogen generation. *J. Phys. Chem. C* 116 (25), 13516–13523. doi:10.1021/jp302146c

Le Gal, A., Abanades, S., and Flamant, G. (2011). CO_2 and H_2O splitting for thermochemical production of solar fuels using nonstoichiometric ceria and ceria/zirconia solid solutions. *Energy fuels.* 25 (10), 4836–4845. doi:10.1021/ef200972r

Lin, F., Samson, V. A., Wismer, A. O., Grolimund, D., Alxneit, I., and Wokaun, A. (2016). Zn-modified ceria as a redox material for thermochemical H_2O and CO_2 splitting: Effect of a secondary ZnO phase on its thermochemical activity. *CrystEngComm* 18, 2559–2569. doi:10.1039/c6ce00430j

Luciani, G., Landi, G., Aronne, A., and Di Benedetto, A. (2018). Partial substitution of B cation in La0.6Sr0.4MnO3 perovskites: A promising strategy to improve the redox properties useful for solar thermochemical water and carbon dioxide splitting. *Sol. Energy* 171, 1–7. doi:10.1016/j.solener.2018.06.058

Marxer, D., Furler, P., Scheffe, J., Geerlings, H., Falter, C., Batteiger, V., et al. (2015). Demonstration of the entire production chain to renewable kerosene via solar thermochemical splitting of H_2O and CO_2. *Energy fuels.* 29 (5), 3241–3250. doi:10.1021/acs.energyfuels.5b00351

McDaniel, A. H., Miller, E. C., Arifin, D., Ambrosini, A., Coker, E. N., O'Hayre, R., et al. (2013). Sr- and Mn-doped $LaAlO_{3-\delta}$ for solar thermochemical H_2 and CO production. *Energy Environ. Sci.* 6 (8), 2424–2428. doi:10.1039/c3ee41372a

Meng, Q., Lee, C., Ishihara, T., Kaneko, H., and Tamaura, Y. (2011). Reactivity of CeO_2-based ceramics for solar hydrogen production via a two-step water-splitting cycle with concentrated solar energy. *Int. J. Hydrogen Energy* 36 (21), 13435–13441. doi:10.1016/j.ijhydene.2011.07.089

Meng, Q-L., and Tamaura, Y. (2014). Enhanced hydrogen production by doping Pr into $Ce_{0.\ 9}Hf_{0.1}O_2$ for thermochemical two-step water-splitting cycle. *J. Phys. Chem. Solids* 75 (3), 328–333. doi:10.1016/j.jpcs.2013.07.023

Miller, J. E., Allendorf, M. D., Diver, R. B., Evans, L. R., Siegel, N. P., and Stuecker, J. N. (2008). Metal oxide composites and structures for ultra-high temperature solar thermochemical cycles. *J. Mat. Sci.* 43 (14), 4714–4728. doi:10.1007/s10853-007-2354-7

Mofijur, M., Atabani, A. E., Masjuki, H. H., Kalam, M. A., and Masum, B. M. (2013). A study on the effects of promising edible and non-edible biodiesel feedstocks on engine performance and emissions production: A comparative evaluation. *Renew. Sustain. Energy Rev.* 23, 391–404. doi:10.1016/j.rser.2013.03.009

Mofijur, M., Masjuki, H. H., Kalam, M. A., and Atabani, A. E. (2013). Evaluation of biodiesel blending, engine performance and emissions characteristics of Jatropha curcas methyl ester: Malaysian perspective. *Energy* 55, 879–887. doi:10.1016/j.energy.2013.02.059

Muhich, C. L., Evanko, B. W., Weston, K. C., Lichty, P., Liang, X., Martinek, J., et al. (2013). Efficient generation of H_2 by splitting water with an isothermal redox cycle. *Science* 341, 540–542. doi:10.1126/science.1239454

Mulmi, S., Chen, H., Hassan, A., Marco, J. F., Berry, F. J., Sharif, F., et al. (2017). Thermochemical CO_2 splitting using double perovskite-type $Ba_2Ca_{0.66}Nb_{1.34-x}$. *J. Mater. Chem. A* 5, 6874–6883. doi:10.1039/C6TA10285A

Mustafa, A., Lougou, B. G., Shuai, Y., Wang, Z., and Tan, H. (2020). Current technology development for CO2 utilization into solar fuels and chemicals: A review. *J. Energy Chem.* 49, 96–123. doi:10.1016/j.jechem.2020.01.023

Nair Mahesh, M., and Abanades, S. (2018). Experimental screening of perovskite oxides as efficient redox materials for solar thermochemical CO_2 conversion. *Sustain. Energy Fuels* 2 (4), 843–854. doi:10.1039/c7se00516d

Nair, M. M., and Abanades, S. (2016). Insights into the redox performance of non–stoichiometric lanthanum manganite perovskites for solar thermochemical CO_2 splitting. *ChemistrySelect* 1 (15), 4449–4457. doi:10.1002/slct.201601171

Nair, M. M., and Abanades, S. (2016). Tailoring Hybrid nonstoichiometric ceria redox cycle for combined solar methane reforming and thermochemical conversion of H_2O/CO_2. *Energy Fuels* 30, 6050–6058. doi:10.1021/acs.energyfuels.6b01063

Parvanian, A. M., Salimijazi, H., Shabaninejad, M., Troitzsch, U., Kreider, P., Lipiński, W., et al. (2020). Thermochemical CO2 splitting performance of perovskite coated porous ceramics. *RSC Adv.* 10, 23049–23057. doi:10.1039/d0ra02353a

Permentier, K., Vercammen, S., Soetaert, S., and Schellemans, C. (2017). Carbon dioxide poisoning: A literature review of an often forgotten cause of intoxication in the emergency department. *Int. J. Emerg. Med.* 10, 14. doi:10.1186/s12245-017-0142-y

Petkovich, N. D., Rudisill, S. G., Venstrom, L. J., Boman, D. B., Davidson, J. H., and Stein, A. (2011). Control of heterogeneity in nanostructured ce1−x zr x o2 binary oxides for enhanced thermal stability and water splitting activity. *J. Phys. Chem. C* 115 (43), 21022–21033. doi:10.1021/jp2071315

Rafique, M., Safdar, N., Irshad, M., Usman, M., Akhtar, M., Saleem, M. W., et al. (2022). Influence of low sintering temperature on $BaCe_{0.2}Zr_{0.6}Y_{0.2}O_{3-\delta}$ IT-SOFC perovskite Electrolyte synthesized by Co-precipitation method. *Materials* 15, 3585. doi:10.3390/ma15103585

Ramos, A. E., Maiti, D., Daza, Y. A., Kuhn, J. N., and Bhethanabotla, V. R. (2019). Co, Fe, and Mn in La-perovskite oxides for low temperature thermochemical CO_2 conversion. *Catal. Today* 338, 52–59. doi:10.1016/j.cattod.2019.04.028

Riaz, A., Ali, M. U., Enge, T. G., Tsuzuki, T., Lowe, A., and Lipiski, W. (2020). Concentration-dependent solar thermochemical CO_2/H_2O splitting performance by vanadia-ceria multiphase metal oxide systems. *Research* 2020, 3049534. doi:10.34133/2020/3049534

Roeb, M., Neises, M., Monnerie, N., Call, F., Simon, H., Sattler, C., et al. (2012). Materials-related aspects of thermochemical water and carbon dioxide splitting: A review. *Materials* 5 (11), 2015–2054. doi:10.3390/ma5112015

Sastre, D., Carrillo, A. J., Serrano, D. P., Pizarro, P., and Coronado, J. M. (2017). Exploring the redox behavior of $La_{0.6}Sr_{0.4}$ $Mn_{1-x}AlxO_3$ perovskites for CO_2-splitting in thermochemical cycles. *Top. Catal.* 60, 1108–1118. doi:10.1007/s11244-017-0790-4

Sastre, D., Carrillo, A. J., Serrano, D. P., Pizarro, P., and Coronado, J. M. (2017). Exploring the redox behavior of $La_{0.6}Sr_{0.4}Mn_{1-x}AlxO_3$ perovskites for CO_2-splitting in thermochemical cycles. *Top. Catal.* 60, 1108–1118. doi:10.1007/s11244-017-0790-4

Scheffe, J. R., Jacot, R., Patzke, G. R., and Steinfeld, A. (2013). Synthesis, characterization, and thermochemical redox performance of Hf^{4+}, Zr^{4+}, and Sc^{3+} doped ceria for splitting CO_2. *J. Phys. Chem. C* 117 (46), 24104–24114. doi:10.1021/jp4050572

Scheffe, J. R., McDaniel, A. H., Allendorf, M. D., and Weimer, A. W. (2013). Kinetics and mechanism of solar-thermochemical H_2 production by oxidation of a cobalt ferrite–zirconia composite. *Energy Environ. Sci.* 6, 963–973. doi:10.1039/c3ee23568h

Scheffe, J. R., and Steinfeld, A. (2014). Oxygen exchange materials for solar thermochemical splitting of H_2O and CO_2: A review. *Mater. Today* 17, 341–348. doi:10.1016/j.mattod.2014.04.025

Scheffe, J. R., Weibel, D., and Steinfeld, A. (2013). Lanthanum–strontium–manganese perovskites as redox materials for solar thermochemical splitting of H_2O and CO_2. *Energy fuels.* 27, 4250–4257. doi:10.1021/ef301923h

Scheffe, J. R., Welte, M., and Steinfeld, A. (2013). "Reduction of cerium dioxide in an aerosol tubular reactor for the thermal dissociation of CO_2 and H_2O," in Paper presented at: Abstracts of Papers of the American Chemical Society, New Orleans, LA, April 7 - 11.

Shahabuddin, M., Alim, M. A., Alam, T., Mofijur, M., Ahmed, S. F., and Perkins, G. (2021). A critical review on the development and challenges of concentrated solar power technologies. *Sustain. Energy Technol. Assessments* 47, 101434. doi:10.1016/j.seta.2021.101434

Snoeckx, R., and Bogaerts, A. (2017). Plasma technology – A novel solution for CO_2 conversion? *Chem. Soc. Rev.* 46, 5805–5863. doi:10.1039/c6cs00066e

Takacs, M., Hoes, M., Caduff, M., Cooper, T., Scheffe, J. R., and Steinfeld, A. (2016). Oxygen nonstoichiometry, defect equilibria, and thermodynamic characterization of $LaMnO_3$ perovskites with Ca/Sr A-site and Al B-site doping. *Acta Mater.* 103, 700–710. doi:10.1016/j.actamat.2015.10.026

Takalkar, G., Bhosale, R. R., AlMomani, F., Rashid, S., Qiblawey, H., Saleh Saad, M. A., et al. (2021). Thermochemical splitting of CO_2 using solution combustion synthesized lanthanum–strontium–manganese perovskites. *Fuel (Lond).* 285, 119154. doi:10.1016/j.fuel.2020.119154

Wang, L., Al-Mamun, M., Liu, P., Wang, Y., Gui Yang, H., and Zhao, H. (2017). $La_{1-x}Ca_xMn_{1-y}Al_yO_3$ perovskites as efficient catalysts for two-step thermochemical water splitting in conjunction with exceptional hydrogen yields. *Chin. J. Catal.* 38 (6), 1079–1086. doi:10.1016/S1872-2067(17)62820-1

Wang, L., Al-Mamun, M., Liu, P., Wang, Y., Yang, H. G., and Zhao, H. (2018). Notable hydrogen production on $La_xCa_{1-x}CoO_3$ perovskites via two-step thermochemical water splitting. *J. Mat. Sci.* 53 (9), 6796–6806. doi:10.1007/s10853-018-2004-2

Wang, L., Al-Mamun, M., Zhong, Y. L., Jiang, L., Liu, P., Wang, Y., et al. (2017). Ca^{2+} and Ga^{3+} doped $LaMnO_3$ perovskite as a highly efficient and stable catalyst for two-step thermochemical water splitting. *Sustain. Energy Fuels* 1 (5), 1013–1017. doi:10.1039/c6se00097e

Wang, L., Al-Mamun, M., Zhong, Y. L., Liu, P., Wang, Y., Yang, H. G., et al. (2018). Enhanced thermochemical water splitting through formation of oxygen vacancy in $La_{0.6}Sr_{0.4}BO_{3-\delta}$ (B=Cr, Mn, Fe, Co, and Ni) perovskites. *Chempluschem* 83 (10), 924–928. doi:10.1002/cplu.201800178

Żaba, C., Marcinkowski, J. T., Wojtyła, A., Tężyk, A., Tobolski, J., and Zaba, Z. (2011). Acute collective gas poisoning at work in a manure storage tank. *Ann. Agric. Environ. Med.* 18, 448

Zhao, B., Huang, C., Ran, R., Wu, X., and Weng, D. (2016). Two-step thermochemical looping using modified ceria-based materials for splitting CO_2. *J. Mat. Sci.* 51 (5), 2299–2306. doi:10.1007/s10853-015-9534-7